TRANSACTIONS ON EMERGING TELECOMMUNICATIONS TECHNOLOGIES
Trans. Emerging Tel. Tech. 2016; **27**:17–33
Published online 22 January 2014 in Wiley Online Library (wileyonlinelibrary.com). DOI: 10.1002/ett.2782

RESEARCH ARTICLE

Joint dynamic switching point configuration and resource allocation in TDD-OFDMA networks: optimal formulation and suboptimal solution

Ahmad M. El-Hajj* and Zaher Dawy

Electrical and Computer Engineering Department, American University of Beirut, Beirut, Lebanon

ABSTRACT

With the large increase in data services with asymmetric traffic loads, the time division duplexing (TDD) mode of operation of the next generation cellular wireless standards has gained an increasing interest from both cellular network operators and the research community. However, the introduction of TDD has raised several critical design requirements. Among others, the introduced flexibility in splitting resources between the uplink and downlink directions makes of the uplink/downlink switching point configuration a major design problem, especially that it is directly connected to other design aspects such as resource allocation and interference mitigation. In this paper, we formulate joint switching point configuration and resource allocation in TDD systems as an optimization problem with the objective of minimising the total interference under traffic load and other network constraints. The problem is then reformulated by linearizing some of the nonlinear terms. Because of the persistent difficulty of the problem, we propose a three-stage suboptimal algorithm. The algorithm clusters the cells in a given network into different groups depending on the susceptibility of cells to interfere on each other with emphasis on base station-base station and mobile station-mobile station interference. Switching point configuration using standardised long term evolution (LTE) frame structures and multicell resource allocation utilising uplink and downlink interference indicators are subsequently performed independently. Simulation results show the merits of the proposed approach compared with traditional techniques by offering attractive trade-offs between interference mitigation and traffic adaptation. Copyright © 2014 John Wiley & Sons, Ltd.

***Correspondence**
Ahmad M. El-Hajj, Electrical and Computer Engineering Department, American University of Beirut, Beirut, Lebanon.
E-mail: ame34@aub.edu.lb

Received 7 August 2013; Revised 6 November 2013; Accepted 27 November 2013

1. INTRODUCTION

The scarcity of available paired spectrum coupled with the emergence of heterogeneous data services with different rate and delay requirements in the uplink and downlink made of time division duplexing (TDD) the technology of choice of many operators around the world. In fact, the deployment of 3G networks and most importantly, Orthogonal Frequency-Division Multiple Access (OFDMA)-based networks has allowed the advent of a plethora of new applications such as voice over internet protocol (VoIP), video conferencing, multiplayer gaming with high quality of service (QoS) requirements in both the uplink and downlink. The addition of these applications to the traditional downlink-based services such as video streaming and web surfing and the uplink-based upload services, creates a significant imbalance between both communication links where the uplink and downlink traffic volumes change from cell to cell in a given network. This has triggered an increased interest in TDD systems.

Compared to frequency division duplexing (FDD) where uplink and downlink occupy different frequency bands, both directions are time multiplexed in TDD, which makes it easier to adjust the amount of resources for uplink and downlink transmission based on network conditions. The other advantages of TDD over FDD include the support for operation in unpaired spectrum, in addition to the inherent characteristics of sharing the same frequency band, which facilitates the use of channel reciprocity in the context of advanced multiple antenna techniques.

The resource management process in TDD-OFDMA networks encompasses two major components: the determination of the switching point configuration and the allocation of the resources taking into account the complexities of the TDD system. The dynamic switching point

Copyright © 2014 John Wiley & Sons, Ltd.

configuration determines whether each slot within a given TDD frame is used for uplink or downlink transmission. The flexibility offered by the dynamic switching point configuration process comes with increased complexities to the scheduling process. In fact, the TDD mode of operation introduces a new type of interference known as *cross-slot interference* as illustrated in Figure 1. A base station (BS) transmitting to a mobile station (MS) in a given cell can interfere on an uplink transmission in a neighbouring cell. With the line of sight (LOS) component usually present between BSs, the induced BS–BS interference, which is usually static, becomes a significant parameter affecting network performance. The other type of cross-slot interference, known as MS–MS interference which is variable occurs when an uplink transmission in one cell interferes on a downlink transmission in another cell. In addition to cross-slot interference, TDD systems suffer from the traditional BS–MS interference in the case of downlink transmission in neighbouring cells and MS–BS interference in case of uplink transmission. Consequently, the resource management intelligence in the network should determine the optimal switching point configuration to reduce interference while satisfying the asymmetric traffic demand requirement in addition to the standard per-slot subcarrier and power allocation.

The various TDD-related challenges were addressed in the literature. Several solutions to TDD-inherited problems are described in [1]. The simplest solution is synchronising transmission over all cells. This eliminates BS–BS and MS–MS interference but reduces the flexibility of dynamic asymmetric allocation. Other solutions include sectorization and timeslot grouping where only users close to the BS are allowed to transmit during cross-slots. An extensive study of TDD wireless land area network systems is provided in [2]. The authors analyse the performance of dynamic switching for both low and high loads. Interference mitigation using busy burst transmission is proposed in [3, 4], and using relaying in [5, 6]. In [7], a priority-based resource allocation algorithm for the downlink of a TDD-OFDMA network that takes into consideration users' priorities, channel and connection quality is presented. In [8], allocation is performed on a slot-by-slot basis by selecting the best modulation scheme and subcarrier allocation to users given the signal-to-noise ratio and the minimum bit error rate required for a users service. Bandwidth allocation schemes that consider uplink and downlink traffic profiles are investigated in [9] and [10]. Finally, in [11], an analytical method is provided to determine the best allocation of resources to the uplink and downlink in order to minimize the blocking rate. Recently, an approach was proposed in [12] to address the problem of adapting TDD frame configurations to the changing uplink and downlink traffic. The scheme used first estimates the required number of resource blocks based on the buffer and arrival data volumes then selects the frame configuration based on the ratio of resource blocks in the uplink and downlink before performing some calibration.

All the presented references consider a solution to a certain aspect of the TDD resource allocation problem such as interference mitigation or uplink/downlink load balance adaptation. The problem of jointly determining the switching point configuration and allocating resources was not treated thoroughly in the literature. Two recent publications stand out in this domain. In [12], TDD frames are configured based on the current arriving and buffered traffic volumes. In [13], different aspects of the dynamic uplink-downlink configuration in TD long-term evolution (LTE) systems are discussed with some preliminary general results. Furthermore, state-of-the-art wireless standards consider a fixed number of possible uplink/downlink con-

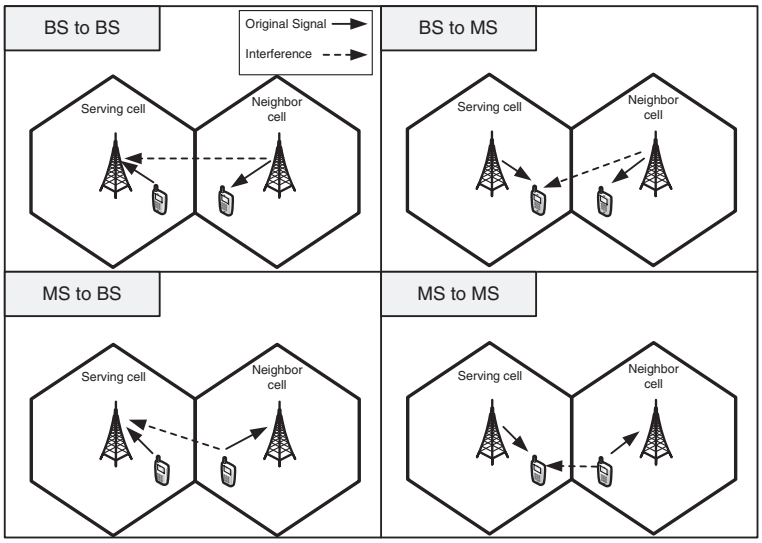

Figure 1. Time division duplexing interference scenarios. Depending in the transmission direction in the adjacent cells, four interference cases can be identified.

Trans. Emerging Tel. Tech. **27**:17–33 (2016) © 2014 John Wiley & Sons, Ltd.
DOI: 10.1002/ett

21613915, 2016, 1, Downloaded from https://onlinelibrary.wiley.com/doi/10.1002/ett.2782 by HINARI-LEBANON, Wiley Online Library on [02/08/2024]. See the Terms and Conditions (https://onlinelibrary.wiley.com/terms-and-conditions) on Wiley Online Library for rules of use; OA articles are governed by the applicable Creative Commons License

figurations where normally one configuration is selected and fixed based on general uplink and downlink traffic forecasts [14].

1.1. Contributions

This work builds up on the work presented in [15]. In [15], joint uplink/downlink resource allocation and switching point configuration were considered for a single cell-OFDMA network. The problem was formulated as a convex optimization problem with the objective taken as a weighted sum of the uplink and downlink sum-rates. The percentages of uplink and downlink resources were determined and updated in an online manner. In this work, the problem of switching point configuration and resource allocation is extended to a multicellular environment where the per-cell uplink and downlink traffic volumes are considered in addition to the different TDD-specific interference cases to jointly determine the optimal switching point configuration and per-slot subcarrier and power allocation. This makes the problem considerably more complex compared with [15] and requiring a new formulation and solution approach that take into account all the parameters affecting the joint dynamic point configuration and resource allocation outcome. The problem is formulated as a mixed integer nonlinear program (MINLP) with the objective of minimising the total interference under traffic and network constraints. Because of the complexity of MINLP problems, linearization techniques are applied to reduce the complexity of the problem and obtain a solution for small to medium networks in an acceptable time. A suboptimal algorithm is also proposed. The dynamic switching point configuration and resource allocation are performed in three stages. A clustering algorithm is first applied to reduce the effect of BS–BS and MS–MS interference. The frame structure is then determined in each cluster given the aggregate traffic requirements in the uplink and downlink. Finally, uplink and downlink resource allocation are performed on a cell-basis based on LTE-specific interference indicators. The proposed suboptimal approach uses the latest interference mitigation and coordination proposals for future generations of the LTE standard, namely, cell clustering interference mitigation and the uplink and downlink interference indicators.

1.2. Paper organisation

The rest of this paper is organised as follows. The system model is presented in Section 2. The joint switching point configuration and resource allocation problem in TDD-OFDMA networks is formulated in Section 3. Section 4 highlights the linearizations applied to the optimization problem. An LTE-oriented suboptimal procedure is described in Section 5. Suboptimal results are presented and analysed in Section 6. Concluding remarks follow in Section 7.

2. SYSTEM MODEL

A multicellular TDD OFDMA-based network is considered. The network is composed of L cells where each cell l has M_l^U uplink flows and M_l^D downlink flows or connections. The transmission frame consists of S slots reserved for uplink or downlink transmission. For instance, in the LTE standard, the frame consists of $S = 10$ slots. Furthermore, the switching point configuration is limited to seven different structures as shown in Figure 2 ([16]). These seven frame structures will be used in Section 5. Depending on the ratio of the uplink to downlink traffic volume, the frame structure with the closest ratio among the seven options is selected. Then, depending on the selected structure, the schedule of uplink and downlink transmission is determined.

The frequency band is divided into K subcarriers where each subcarrier is exclusively allocated to one user per cell for uplink or downlink transmission according to the frame switching point configuration. Let $w_{i,j,l,s}^U$ and $w_{i,j,l,s}^D$

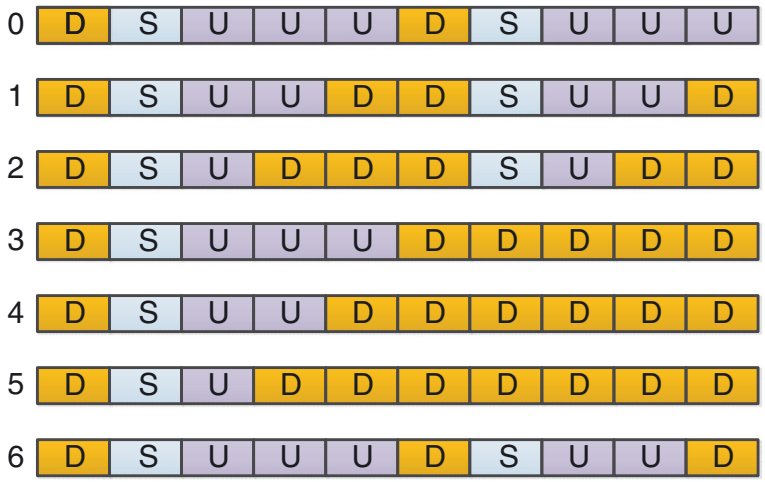

Figure 2. Time division long-term evolution frame structures (D, downlink; U, uplink; S, special subframe).

21613915, 2016, 1, Downloaded from https://onlinelibrary.wiley.com/doi/10.1002/ett.2782 by HINARI-LEBANON, Wiley Online Library on [02/08/2024]. See the Terms and Conditions (https://onlinelibrary.wiley.com/terms-and-conditions) on Wiley Online Library for rules of use; OA articles are governed by the applicable Creative Commons License

be the subcarrier allocation indices denoting whether subcarrier j is allocated to user i in cell l and slot s in the uplink and downlink, respectively. Let $p^U_{i,j,l,s}$ and $p^D_{i,j,l,s}$ be the power allocated on that subcarrier in the uplink and downlink, respectively. The power budget of user i is limited to $P^U_{\max,i}$, and the power budget of the BS is set to P^D_{BS}. Finally, $t_{l,s}$ is a binary variable denoting whether cell l is configured for uplink transmission ($t_{l,s} = 0$) or downlink transmission ($t_{l,s} = 1$) in slot s. The channel model depends on the transmitting and receiving entities. $\gamma^{i,j,s,x,l}_{\mathrm{BS-BS}}$ denotes the channel loss in the downlink transmission of user i on subcarrier j and slot s from the BS in cell x to that in cell l. $\gamma^{i,j,x,s,o,l}_{\mathrm{MS-MS}}$ denotes the channel loss in the uplink transmission by user i on subcarrier j and slot s from cell x to user o in cell l. $\gamma^{i,j,x,s,o,l}_{\mathrm{BS-MS}}$ is the channel loss in the downlink transmission of user i on subcarrier j and slot s from the BS in cell x to MS o in cell l. Finally, $\gamma^{i,j,s,x,l}_{\mathrm{MS-BS}}$ denotes the channel loss in the uplink transmission by user i on subcarrier j and slot s in cell x to the BS in cell l. The channel loss is modelled using the combined effect of pathloss and fading. A pathloss model is used for all connections; however, the model varies depending on the transmitting and receiving entities. For the BS–BS link, a simplified pathloss model is assumed with a pathloss exponent of two. According to [17], the pathloss (PL) is given as $\mathrm{PL}(d) = 98.45 + 20\log_{10}(d)$ where d is the distance in kilometres. For the MS–MS link, a pathloss model known as the Xia model is also assumed and considers outdoor MSs. For an MS–MS distance smaller than 50 m, the pathloss (PL) is given as $\mathrm{PL}(d) = 98.45 + 20\log_{10}(d)$ where d is the distance in kilometres. Otherwise, it is given as $\mathrm{PL}(d) = 175.78 + 40\log_{10}(d)$. Finally, for the BS–MS, link, the pathloss expression is given as $\mathrm{PL}(d) = 128.1 + 37.6\log_{10}(d)$. We also assume Rayleigh fading, hence, the channel gain is exponentially distributed with mean equal to the path gain.

3. PROBLEM FORMULATION

The objective of the problem is to minimize the total interference in the network subject to the varying traffic load constraints in addition to the power and subcarrier allocation constraints. Interference was chosen as the main parameter to optimise because it affects network performance in terms of coverage, capacity and throughput. High interference usually undermines the achievable throughput and causes severe performance deterioration. However, the relation between throughput and interference is not linear especially in TDD systems where uplink and downlink are time-multiplexed and where different types of interference exist with varying impact. At the same time, traffic and rate requirements necessitate a certain per-user uplink and downlink rate thus implying a positive or a negative effect from one cell over the other. Thus, interference is chosen as the objective to be minimized under traffic constraint in order to try and find the best trade-off in network performance through an optimised management of the resources (slot configuration, subcarrier and power allocation).

In fact, the general formulation of the objective function is given as

$$\min_{\mathbf{t},\mathbf{w},\mathbf{p}} \frac{1}{S}\sum_{s=1}^{S}\sum_{l=1}^{L}\sum_{x\neq l}\alpha_1 I^{x,l,s}_{\mathrm{BS-BS}}(\mathbf{t},\mathbf{w},\mathbf{p}) + \alpha_2 I^{x,l,s}_{\mathrm{BS-MS}}(\mathbf{t},\mathbf{w},\mathbf{p}) + \alpha_3 I^{x,l,s}_{\mathrm{MS-MS}}(\mathbf{t},\mathbf{w},\mathbf{p}) + \alpha_4 I^{x,l,s}_{\mathrm{MS-BS}}(\mathbf{t},\mathbf{w},\mathbf{p}) \tag{1}$$

where $I^{x,l,s}_{\mathrm{BS-BS}}$ is the BS–BS interference from cell x on cell l in slot s as a function of the vectors of variables $(\mathbf{t},\mathbf{w},\mathbf{p})$. The BS–MS interference term $I_{\mathrm{BS-MS}}$, MS–MS interference $I_{\mathrm{MS-MS}}$ and MS–BS interference $I_{\mathrm{MS-BS}}$ are defined accordingly. $\alpha_1,\cdots,\alpha_4$ are weighting constants such as $\sum_{i=1}^{4}\alpha_i = 1$.

When all terms have equal weights,that is, $\alpha_i = \frac{1}{4} \quad i = 1,\cdots,4$, the formulation in (1) is equivalent to minimising the total interference in the network. On the other hand, if one type of interference is considered, the outcome of the dynamic frame configuration process would be different because it will be biased towards the factors affected by that type of interference. For instance, in case BS–BS interference is only considered, that is, $\alpha_1 = 1$, the dynamic configuration process would be biased towards avoiding concurrent uplink and downlink cross-slots to be assigned in the BSs of a given network. In such a case, and because BS–BS interference is the highest among all types of interference, this will bias the solution towards a fully synchronised one.

Hence, the interference minimization framework is flexible and can accommodate several objectives depending on the requirements of the network design. In this paper, we consider the minimization of the total interference with equal weights. The joint multicell TDD dynamic switching point configuration and resource allocation problem can therefore be formulated using Equations (2)–(7):

$$\begin{aligned}\min_{\mathbf{t},\mathbf{w},\mathbf{p}} \frac{1}{S}\sum_{s=1}^{S}\sum_{l=1}^{L}\Bigg(\sum_{x\neq l}\Bigg((1-t_{l,s})t_{x,s}\sum_{j=1}^{K}\sum_{i=1}^{M^D_x} w^D_{i,j,x,s}p^D_{i,j,x,s}\cdot\gamma^{i,j,s,x,l}_{\mathrm{BS-BS}} \\ + t_{l,s}(1-t_{x,s})\sum_{j=1}^{K}\sum_{o=1}^{M^D_l} w^D_{o,j,l,s}\sum_{i=1}^{M^U_x} w^U_{i,j,x,s}p^U_{i,j,x,s}\cdot\gamma^{i,j,x,s,o,l}_{\mathrm{MS-MS}} \\ + t_{l,s}t_{x,s}\sum_{j=1}^{K}\sum_{o=1}^{M^D_l} w^D_{o,j,l,s}\sum_{i=1}^{M^D_x} w^D_{i,j,x,s}p^D_{i,j,x,s}\cdot\gamma^{i,j,x,s,o,l}_{\mathrm{BS-MS}} \\ +(1-t_{l,s})(1-t_{x,s})\sum_{j=1}^{K}\sum_{i=1}^{M^U_x} w^U_{i,j,x,s}p^U_{i,j,x,s}\cdot\gamma^{i,j,s,x,l}_{\mathrm{MS-BS}}\Bigg)\Bigg)\end{aligned} \tag{2}$$

subject to

$$\frac{R^U_l}{R^D_l} = \theta_l \ \forall l \tag{3}$$

Trans. Emerging Tel. Tech. **27**:17–33 (2016) © 2014 John Wiley & Sons, Ltd.
DOI: 10.1002/ett

21613915, 2016, 1, Downloaded from https://onlinelibrary.wiley.com/doi/10.1002/ett.2782 by HINARI-LEBANON, Wiley Online Library on [02/08/2024]. See the Terms and Conditions (https://onlinelibrary.wiley.com/terms-and-conditions) on Wiley Online Library for rules of use; OA articles are governed by the applicable Creative Commons License

$$\sum_{j=1}^{K} p^{U}_{i,j,l,s} \leqslant P^{U}_{\max,i} \ \forall i,l,s \quad \sum_{i=1}^{M^{D}_{l}} \sum_{j=1}^{K} p^{D}_{i,j,l,s} \leqslant P^{D}_{\mathrm{BS}} \ \forall l,s \tag{4}$$

$$\sum_{i=1}^{M^{U}_{l}} w^{U}_{i,j,l,s} \leqslant 1 \ \forall j,l,s \quad \sum_{i=1}^{M^{D}_{l}} w^{D}_{i,j,l,s} \leqslant 1 \ \forall j,l,s \tag{5}$$

$$t_{l,s} \in \{0,1\} \ \forall l,s \tag{6}$$

$$w_{i,j,l,s} \in \{0,1\} \ \forall i,j,l,s \tag{7}$$

where the rates in the uplink and downlink are given in (8) and (9), respectively.

The optimization variables include the vector of slot configuration $\mathbf{t}$ where each element corresponds to the status of a given slot s in a cell l. The other variables are the vectors $\mathbf{w}$ and $\mathbf{p}$ of subcarrier and power allocation indices. The objective function in (2) includes four terms to account for the four TDD interference scenarios. The first term in (2) accounts for the BS–BS interference. In a given cell, it is modelled as the total power received from neighbouring cells, which are in downlink transmission given that the reference cell is in uplink transmission. Hence, the factor $(1 - t_{l,s})t_{x,s}$ in the first part of the objective function ensures this condition. For instance, if $t_{x,s} = 0$, indicating uplink transmission in the neighbouring cell, then the BS–BS interference will be equal to zero. Similar reasoning applies if the reference cell is in downlink transmission ($(1 - t_{l,s}) = 0$). The received power is given as the sum of the attenuated received power from all downlink $\left(M^{D}_{x}\right)$ in the neighbouring cells. The second term in (2) deals with MS–MS interference, which is modelled as follows. For each downlink transmission in the reference cell, the power received from neighbouring uplink transmissions on the same subcarrier are added together. Again, the factor $t_{l,s}(1 - t_{x,s})$ is included to capture the cases where the reference cell is used for downlink transmission, whereas the other cells are configured for uplink transmission. The third term in (2) models the BS–MS interference. For each downlink transmission in the reference cell, the downlink received power over the same subcarrier from the neighbouring BSs are added together. Note that in the formulation, the summation is for all downlink flows in the neighbouring cells but because a subcarrier is exclusively allocated to one user, $w^{D}_{i,j,x,s}$ would be equal to zero for all users except one. Finally, the last term in the objective similarly models the MS–BS interference. The four types of interference are summed over the L cells and averaged over a frame duration (S slots).

The rate constraint in (3) provides one of the alternatives to account for the asymmetrical traffic volumes. The ratio of the uplink to the downlink total cell rate is compared with a certain traffic constant θ_l. The constant is normally determined by evaluating the aggregate uplink and downlink traffic volumes in a given cell, then finding their ratio. This models the traffic differences between the uplink and downlink at a certain scheduling instance. Note that in this paper, the focus is only on emulating traffic variations (without service differentiation) to test their impact on the joint resource allocation and switching point configuration process. Consequently, the rate ratio constraint was added without any minimum rate constraint.

The rates in the uplink and downlink are given in (8) and (9), respectively. The uplink rate is calculated for a given cell and averaged over all uplink time slots. As shown in (8), the two interference terms in the rate expression are the BS–BS and MS–BS interference from the neighbouring cells. The downlink rate expression in (9) is similar to the uplink one but accounts for BS–MS and MS–MS interference. The power constraints in (4) mandate that the power allocated for a given user's uplink transmission and for all downlink transmissions within a given cell to be below the power budget of the MS and BS, respectively. Subcarrier allocation constraints are included in (5). These constraints relax the exclusive subcarrier allocation requirement to account for time sharing among users in order to reduce the complexity of the problem. Finally, the slot configuration constraints are provided in (6) to check whether a cell is used for uplink or downlink is a given slot.

The formulated problem belongs to the class of MINLP problems. The difficulty in such problems is associated with the nature of the problem, namely, the combinatorial domain (binary variables domain) and the continuous domain. More specifically, the large number of binary variables makes the problem NP-complete [18].

$$R^{U}_{l} = \frac{1}{S} \sum_{i=1}^{M^{U}_{l}} \sum_{s=1}^{S} (1 - t_{l,s}) \sum_{j=1}^{K} w^{U}_{i,j,l,s} \log \left(1 + \frac{p^{U}_{i,j,l,s} \gamma^{i,j,s,l,l}_{\mathrm{MS-BS}}}{\sigma^2 + \sum_{x \neq l} \left(t_{x,s} \sum_{o=1}^{M^{D}_{x}} w^{D}_{o,j,x,s} p^{D}_{o,j,x,s} \gamma^{o,j,s,x,l}_{\mathrm{BS-BS}} + (1 - t_{x,s}) \sum_{o=1}^{M^{U}_{x}} w^{U}_{o,j,x,s} p^{U}_{o,j,x,s} \gamma^{o,j,s,x,l}_{\mathrm{MS-BS}} \right)} \right) \tag{8}$$

$$R^{D}_{l} = \frac{1}{S} \sum_{i=1}^{M^{D}_{l}} \sum_{s=1}^{S} t_{l,s} \sum_{j=1}^{K} w^{D}_{i,j,l,s} \log \left(1 + \frac{p^{D}_{i,j,l,s} \gamma^{D}_{i,j,l,s}}{\sigma^2 + \sum_{x \neq l} \left(t_{x,s} \sum_{o=1}^{M^{D}_{x}} w^{D}_{o,j,x,s} p^{D}_{o,j,x,s} \gamma^{i,j,x,s,o,l}_{\mathrm{BS-MS}} + (1 - t_{x,s}) \sum_{o=1}^{M^{U}_{x}} w^{U}_{o,j,x,s} p^{U}_{o,j,x,s} \gamma^{i,j,x,s,o,l}_{\mathrm{MS-MS}} \right)} \right) \tag{9}$$

21613915, 2016, 1, Downloaded from https://onlinelibrary.wiley.com/doi/10.1002/ett.2782 by HINARI-LEBANON, Wiley Online Library on [02/08/2024]. See the Terms and Conditions (https://onlinelibrary.wiley.com/terms-and-conditions) on Wiley Online Library for rules of use; OA articles are governed by the applicable Creative Commons License

4. PROBLEM REFORMULATION

The problem as formulated in (2) is difficult to solve even for small cell networks. Therefore, we perform some linearization to the problem by using the approach presented in [19]. The procedure involves replacing nonlinear terms in the objective and constraints with new variables and new constraints. The approach yields a new optimization problem with a larger number of variables and constraints but with a smaller amount of nonlinearities. This makes the problem solvable using some known algorithms such as the outer approximation algorithm [20]. For illustration purposes, we show the linearization outcome for the first term in the objective function that is, $\sum_{s=1}^{S}\sum_{l=1}^{L}\sum_{x\neq l}(1-t_{l,s})t_{x,s}\sum_{j=1}^{K}\sum_{i=1}^{M_x^D} w_{i,j,x,s}^{D} p_{i,j,x,s}^{D}\gamma_{\mathrm{BS-BS}}^{i,j,s,x,l}$, which is composed of the sum of $2SL(L-1)KM$ terms of the form $cx_1x_2\cdots x_n y$ where c is a constant, $x_1,\cdots,x_n$ are binary variables and y is a continuous variable. For instance, consider the term $t_{x,s}w_{i,j,x,s}^{D}p_{i,j,x,s}^{D}\gamma_{\mathrm{BS-BS}}^{i,j,s,x,l}$ where $\gamma_{\mathrm{BS-BS}}^{i,j,s,x,l}$ is the constant term, $p_{i,j,x,s}^{D}$ is a continuous variable, $t_{x,s}$ and $w_{i,j,x,s}^{D}$ are binary variables. Because the constant is positive and the non-linear term appears in the objective function, the non-linear term belongs to the first class in [19]. It is replaced by a continuous variable $z_{i,j,x,l,s}^{\mathrm{BS-BS}}$ and the two constraints $z_{i,j,x,l,s}^{\mathrm{BS-BS}} \geqslant \gamma_{\mathrm{BS-BS}}^{i,j,s,x,l}p_{i,j,x,s}^{D} - \gamma_{\mathrm{BS-BS}}^{i,j,s,x,l}P_{\mathrm{BS}}^{D}\left(2-t_{x,s}-w_{i,j,x,s}^{D}\right)$ and $z_{i,j,x,l,s}^{\mathrm{BS-BS}} \geqslant 0$. A similar analysis can be performed for the term $-t_{l,s}t_{x,s}w_{i,j,x,s}^{D}p_{i,j,x,s}^{D}\gamma_{\mathrm{BS-BS}}^{i,j,s,x,l}$ where in this case the constant term $-\gamma_{\mathrm{BS-BS}}^{i,j,s,x,l}$ is negative.

Finally, this equation can be rewritten using the following terms and associated constraints.

$$\sum_{s=1}^{S}\sum_{l=1}^{L}\sum_{x\neq l}\sum_{j=1}^{K}\sum_{i=1}^{M_x^D} z_{i,j,x,l,s}^{\mathrm{BS-BS}} + y_{i,j,x,l,s}^{\mathrm{BS-BS}} \tag{10}$$

Constraints

$$z_{i,j,x,l,s}^{\mathrm{BS-BS}} \geqslant \gamma_{\mathrm{BS-BS}}^{i,j,s,x,l}p_{i,j,x,s}^{D} - \gamma_{\mathrm{BS-BS}}^{i,j,s,x,l}P_{\mathrm{BS}}^{D}\left(2-t_{x,s}-w_{i,j,x,s}^{D}\right) \tag{11}$$

$$z_{i,j,x,l,s}^{\mathrm{BS-BS}} \geqslant 0 \tag{12}$$

$$\begin{aligned} y_{i,j,x,l,s}^{\mathrm{BS-BS}} \geqslant & \gamma_{\mathrm{BS-BS}}^{i,j,s,x,l}P_{\mathrm{BS}}^{D}\left(t_{l,s}+t_{x,s}+w_{i,j,x,s}^{D}-3\right) \\ & - \gamma_{\mathrm{BS-BS}}^{i,j,s,x,l}p_{i,j,x,s}^{D} \end{aligned} \tag{13}$$

$$y_{i,j,x,l,s}^{\mathrm{BS-BS}} \geqslant -\gamma_{\mathrm{BS-BS}}^{i,j,s,x,l}P_{\mathrm{BS}}^{D}k_{i,j,x,l,s}^{1} \tag{14}$$

$$k_{i,j,x,l,s}^{1} \leqslant \frac{1}{3}\left(t_{l,s}+t_{x,s}+w_{i,j,x,s}^{D}\right) \tag{15}$$

$$k_{i,j,x,l,s}^{1} \geqslant \frac{1}{3}\left(t_{l,s}+t_{x,s}+w_{i,j,x,s}^{D}\right) - \frac{2}{3} \tag{16}$$

Equation (10) replaces the BS–BS interference part of the objective function. The two new *continuous variables* are $z_{i,j,x,l,s}^{\mathrm{BS-BS}}$ and $y_{i,j,x,l,s}^{\mathrm{BS-BS}}$ where the former corresponds to terms with a positive constant and the latter to terms with a negative constant value. Constraints (11)–(12) and (13)–(16) correspond to $z_{i,j,x,l,s}^{\mathrm{BS-BS}}$ and $y_{i,j,x,l,s}^{\mathrm{BS-BS}}$, respectively. They are added to ensure that the solution of the reformulated problem is equivalent to the original one. The reformulation introduces some new variables such as $k_{i,j,x,l,s}^{1}$, which is a *binary variable*. More details about the equivalence of the two optimization formulations can be found in [19]. The same approach is applied to the other nonlinear terms in the objectives and constraints. Note that for the constraint, the reformulation of the terms does not lead to fully linear expressions because of the presence of the logarithm in the throughput formula.

The linearized problem can be solved using the AIMMS® solver, which utilises a version of the outer approximation algorithm [21]. The solver combines the merits of two other solvers, which are CONOPT for nonlinear programs and CPLEX for mixed integer problems.

To illustrate the optimal solution, we consider a small network with five hexagonally shaped cells with a 1000 m radius. We also assume BSs with omnidirectional antennas placed at the centre of the cells. In each cell, we consider a TDD-OFDMA frame structure with $S = 6$ slots to be configured for uplink or downlink transmission and $K = 7$ subcarriers to be allocated among three users in each cell. In (3), $\theta = [0.5, 2, 1, 0.1, 9]$. Finally, the power budget of the users is $P_{\max} = 125$ mW and the power budget of each of the BSs is $P_{\mathrm{BS}} = 30$ W. The channel variations assume the pathloss and fading models described in Section 2.

The problem corresponding to this network was solved to completion using AIMMS. The solver takes 2803.98 s to reach a solution. The running time is large given the network size; however, it is reasonable when the high number of binary and continuous variables is considered. In fact, looking at the problem statistics in the solver, the number of variables is 134851 and that of the constraints is 318071. These numbers reflect the difficulty of obtaining the optimal solution for medium to large networks.

The resulting switching point configuration is shown in Table I. In the table, a 0 refers to an uplink transmission and 1 to the downlink one. We can note that a lot of the slots are synchronised to mitigate the effect of BS–BS and MS–MS interference. However, because of the different traffic requirements, some cross-slots do exist. For instance, in

Table I. Per-cluster frame structures.

Cell index \ slot index	1	2	3	4	5	6
1	1	0	0	1	0	1
2	1	0	0	1	0	0
3	1	0	0	1	0	0
4	1	0	0	1	0	0
5	0	0	0	1	0	0

Trans. Emerging Tel. Tech. **27**:17–33 (2016) © 2014 John Wiley & Sons, Ltd.
DOI: 10.1002/ett

21613915, 2016, 1, Downloaded from https://onlinelibrary.wiley.com/doi/10.1002/ett.2782 by HINARI-LEBANON, Wiley Online Library on [02/08/2024]. See the Terms and Conditions (https://onlinelibrary.wiley.com/terms-and-conditions) on Wiley Online Library for rules of use; OA articles are governed by the applicable Creative Commons License

cell 5, only one slot is scheduled for downlink transmission. This is because of the fact for that particular cell, the required uplink traffic is nine times the downlink one. Similarly, the first cell has three slots dedicated for downlink transmission.

5. LTE-ORIENTED SUBOPTIMAL ALGORITHM

The formulated joint dynamic switching point configuration and resource allocation optimization problem in addition to the linearized version are difficult to solve and not scalable to large networks. In this section, we present a suboptimal solution that utilises clustering concepts in addition to LTE signalling techniques based on full/cluster-based coordination between the BS over the X2 interface (More details about the X2 interface can be found in [22] and [23, Chapter 5]).

The proposed approach is composed of three stages. First, the BSs are clustered into different scheduling groups. The idea here is to provide an intermediate solution between fully dynamic switching point configuration as was performed in the proposed optimization formulation and complete network synchronisation where all the cells adopt the same frame structure regardless of the traffic condition differences; complete network synchronisation is the widely adopted solution for (time division) TD-LTE networks [14]. As a result, the frame configurations are synchronised within each cluster and can differ from cluster to cluster. The main metric for cluster formation is the inverse of a weighted combination of the BS–BS interference and the worst case MS–MS interference. Note that cell cluster interference mitigation was mentioned as a possible enhancement technique for LTE [17]. The second stage consists of determining the switching point configuration. This is carried out by considering the aggregate downlink and uplink traffic in all cells belonging to a single cluster. The switching point configurations are selected from the seven configuration supported by the LTE standard [24] (Figure 2). The last stage revolves around the per-cell uplink and downlink resource allocation. The procedure utilises interference indicators such as the high interference indication (HII) for the uplink and the relative narrowband transmit power (RNTP) for the downlink [16, 22].

5.1. Stage 1: Cell cluster interference mitigation

The first step in the approach is to perform interference mitigation through cell clustering. The idea is to divide the scheduling domain into smaller sub-domains. The main metric used is a function of the combination of the BS–BS interference and the worst case MS–MS interference. The BS–BS constitutes the major source of interference because of the LOS component of the transmission between the BSs in addition to the high power budget available for downlink transmission. It is also a fixed source of interference because the locations of BSs are usually fixed. On the other hand, the sources of MS–MS interference are variable and involve NLOS transmission; therefore, because MS–MS interference is usually the lowest among all interference scenarios in TDD systems, we consider the worst case MS–MS interference between two cells in the metric calculation. The distance metric between cells i and j is therefore given by

$$\delta_{i,j} = I_{i,j}^{-1} = \left(\lambda I_{\mathrm{BS}_i,\mathrm{BS}_j} + (1-\lambda) I_{\mathrm{MS}_i,\mathrm{MS}_j}^{\mathrm{worst}}\right)^{-1} \quad (17)$$

where the interference between BS i and BS j, $I_{\mathrm{BS}_i,\mathrm{BS}_j}$, and the worst case MS–MS interference between cells i and j, $I_{\mathrm{MS}_i,\mathrm{MS}_j}^{\mathrm{worst}}$, are calculated assuming transmission with maximum power in the downlink and uplink, respectively. $I_{\mathrm{MS}_i,\mathrm{MS}_j}^{\mathrm{worst}}$ was calculated by finding the interference caused by all MSs in one cell on another cell then selecting the maximum value. The clustering metric is then the inverse of the total interference. As the interference between two cells is larger, the distance between them is smaller because we would like to group them in the same cluster and synchronise the frame configuration between them. The weight given to BS–BS and worst-case MS–MS interference can be modified through the factor λ. For instance, a λ value of 1 means that the clustering is only based on BS–BS interference. The approach requires the knowledge of the channel quality between all entities in the network. In real networks, the calculation of the interference values can be carried out using channel quality estimates in the uplink and downlink.

After calculating the interference metric between BSs in the network, clustering is performed using hierarchical agglomerative clustering (HAC). This class of clustering algorithms starts by considering single element clusters. Clusters are then combined according to a similarity or dissimilarity function [25]. The matrix theory-based HAC algorithm can be outlined as follows [25]:

- **Notations**: Let $\Xi = \{\xi_n, n = 1, \cdots N\}$ be a set of vectors to be clustered. Let $\mathfrak{R}$ be a clustering where $\mathfrak{R} = \{\mathfrak{C}_q, q = 1, \cdots m\}$ and $\mathfrak{C}_q \subseteq \Xi$. $\mathfrak{P}(\Xi)$ is known as the (dis)similarity matrix where each entry denotes the similarity or dissimilarity between two vectors. Finally, let $\mathrm{dist}(\mathfrak{C}_q, \mathfrak{C}_b)$ denote the distance between clusters q and b
- **Initialization**:
  - $\mathfrak{R}_0 = \{\{\xi_n\}, n = 1, \cdots N\}$
  - $\mathfrak{P}_0 = \mathfrak{P}(\Xi)$
  - $\mathrm{it} = 0$
- **Repeat**:
  - $\mathrm{it} = \mathrm{it} + 1$
  - Find $\mathfrak{C}_q$, $\mathfrak{C}_b$ such that $\mathrm{dist}(\mathfrak{C}_q, \mathfrak{C}_b)$ is the minimum distance between two clusters among all clusters

21613915, 2016, 1, Downloaded from https://onlinelibrary.wiley.com/doi/10.1002/ett.2782 by HINARI-LEBANON, Wiley Online Library on [02/08/2024]. See the Terms and Conditions (https://onlinelibrary.wiley.com/terms-and-conditions) on Wiley Online Library for rules of use; OA articles are governed by the applicable Creative Commons License

- Merge $\mathfrak{C}_q$, $\mathfrak{C}_b$ into a single cluster $\mathfrak{C}_{\text{new}}$ and form $\mathfrak{R}_{\text{it}} = (\mathfrak{R}_{\text{it}-1} - \{\mathfrak{C}_q,\ \mathfrak{C}_b\}) \cup \{\mathfrak{C}_{\text{new}}\}$
- Generate $\mathfrak{P}_{\text{it}}$ from $\mathfrak{P}_{\text{it}-1}$ by performing some row and column operations to remove information of the deleted clusters and calculate distances between the new cluster and the other clusters

- **Termination**: Terminate when clustering $\mathfrak{R}_{N-1}$ is formed

The algorithm produces a hierarchy of clusterings represented using a dendrogram. By cutting the dendrogram at a given level, an outcome is produced. Note that the HAC algorithm accommodates different distance measures. In this work, we use the unweighted pair group method average metric where the distance measure is given by

$$d(\mathfrak{C}_q, \mathfrak{C}_b) = \frac{1}{N_q N_b} \sum_{n_q=1}^{N_q} \sum_{n_b=1}^{N_b} \text{dist}(\xi_{q,n_q}, \xi_{b,n_b}) \qquad (18)$$

where N_q and N_b are the cardinalities of $\mathfrak{C}_q$ and $\mathfrak{C}_b$, respectively. ξ_{q,n_q} refers to the n_q^{th} vector in cluster $\mathfrak{C}_q$.

5.2. Stage 2: Switching point configuration

After dividing the set of BSs into separate clusters, the frame configuration is determined. In contrast to the optimization framework where resource allocation and dynamic switching point configuration are jointly optimised at the same time, the frame configuration in the suboptimal solution is determined solely based on the uplink and downlink traffic loads, which is the method used in practical LTE networks. In real networks, frame structures are synchronised among BSs where synchronisation is satellite-based or according to an external time reference [14].

In this work, we assume that only cells belonging to the same cluster have synchronised switching point configurations. Therefore, to find the appropriate frame structure, the aggregate downlink and uplink traffic volumes in all cells is considered. The downlink to uplink traffic ratio is determined and the appropriate switching point configuration is selected among the seven frame structures supported in the LTE standard and shown in Figure 2. Compared with the dynamic approach, the switching is determined regardless of the resource allocation process. Furthermore, for a given configuration and traffic ratio, the order of uplink and downlink transmissions is predetermined in a given frame. The main advantage over the synchronised network solution is that the synchronisation penalty in terms of traffic adaptation is limited to cells belonging to the same cluster rather than the whole network.

5.3. Stage 3: Resource allocation

After determining the switching point configuration within each cluster of the TDD network, the last stage involves performing multicell resource allocation in the network. Usually, resource allocation and switching point configuration are interrelated as was carried out in the joint optimization formulation. However, because of the high complexity of the joint solution especially for medium to large sized networks, the resource allocation is performed independently on a subframe basis in the suboptimal approach. The proposed resource allocation algorithm is based on the uplink multicell approach presented in [26]. However, the technique is adapted to benefit from the interference indicators introduced in the LTE standard [22].

(a) *Utility definition:* The bulk of the resource allocation algorithm lies in the utility definition. In contrast to the optimal formulation, the utility is defined here at the user level. This is because of the fact that the switching point configuration has been determined in the previous stages of the suboptimal algorithm.

The resource allocation is performed on a cell-basis. For a given user i, a given subcarrier j and a link direction (uplink or downlink), the utility in cell l in subframe s is defined as follows:

$$\Gamma_{i,j,l,s} = \beta_{i,j,l,s} R_{i,j,l,s} \qquad (19)$$

where $\beta_{i,j,l,s}$ is a weighting factor and $R_{i,j,l,s}$ is the rate of user i on subcarrier j in cell l and subframe s. The interference information will be incorporated in the weighting factor rather than the rate expression and this is because, as it will be explained later, of the fact that interference information is quantized in the LTE standard.

(b) *Weighting factor:* The weighting factor is included in the utility expression to bias the resource allocation process according to interference information exchanged between BSs. The definition of the weights depends on the level of coordination that exists between the BSs. This work will treat two particular cases. The first assumes full synchronisation (fc) between all cells in all clusters. The TDD network is then assimilated to a mesh network where each cell exchanges information with all other cells. The second case assumes only coordination between cells belonging to the same cluster (cc). In such a case, the network is considered as a group of isolated scheduling islands where the effect of BS–BS and MS–MS interference between cells of different clusters are not taken into account in the scheduling process. Another alternative would be by considering a separate frequency subband for each of the clusters.

The derivation of the weights depends on two LTE interference indicators, RNTP for the downlink and HII for the uplink. RNTP is a downlink indicator exchanged between BSs on the X2 interface. Each bit

Trans. Emerging Tel. Tech. **27**:17–33 (2016) © 2014 John Wiley & Sons, Ltd.
DOI: 10.1002/ett

21613915, 2016, 1, Downloaded from https://onlinelibrary.wiley.com/doi/10.1002/ett.2782 by HINARI-LEBANON, Wiley Online Library on [02/08/2024]. See the Terms and Conditions (https://onlinelibrary.wiley.com/terms-and-conditions) on Wiley Online Library for rules of use; OA articles are governed by the applicable Creative Commons License

of the RNTP indicator corresponds to one resource block in the frequency domain and is used to inform the neighbouring BSs if a cell is planning to keep the transmit power for the resource block (RB) below a certain upper limit or not [16]. This will inform receiving BSs to avoid scheduling users near the transmitting BS on that RB. The second indicator is the HII indicator and used for uplink interference coordination. Similarly to RNTP, a value of one for a given RB indicates high interference sensitivity and a value of zero indicating low interference sensitivity [22].*Without loss of generality, we assume that the HII and RNTP indicators are available on a subcarrier basis rather than resource blocks. Note that, even if the indicators are standardized, the way to use them in the scheduling process is left open for research.*

For the full BS coordination case, some of the cells are scheduled for uplink transmission and others for downlink in a given subframe. Let L_U and L_D denote the number of cells scheduled for uplink and downlink transmission in a given slot, respectively. The weight in the full coordination case is given by

$$\beta^{\mathrm{fc}}_{i,j,l,s}=\left(\prod_{u=1,u\neq l}^{L_U}\left(d_{\mathrm{MS}_{i,l},\mathrm{BS}_u}\right)^{\mathrm{HII}_{j,u}}\prod_{e=1,e\neq l}^{L_D}\left(d_{\mathrm{MS}_{i,l},\mathrm{BS}_e}\right)^{\mathrm{RNTP}_{j,e}}\right)^{1/L} \tag{20}$$

where $d_{\mathrm{MS}_{i,l},\mathrm{BS}_u}$ is the distance between user i in cell l and the BS of cell u. The term $\left(d_{\mathrm{MS}_{i,l},\mathrm{BS}_u}\right)^{\mathrm{HII}_{j,u}}$ is equal to 1 if a low uplink interference indication is received on subcarrier j from cell u, that is, $\mathrm{HII}_{j,u}=0$ and is equal to $d_{\mathrm{MS}_{i,l},\mathrm{BS}_u}$ otherwise. The significance of this term is that for high interference indication received, we would like to favour users with high distance from the BS, either to reduce interference for uplink transmission, and to decrease the chances of suffering high interference in case of a downlink transmission. The downlink terms with the RNTP indicator have an analogous interpretation to the uplink case. Finally, the weight for each user on a given subcarrier is the geometric mean of all distance terms from all cells. Thus, a user that is the most likely to cause or suffer the least interference on a given subcarrier will have the largest weight for it.

For the cluster coordination case, we neglect the effect of BS–BS and MS–MS interference from cells that do not belong to a given cluster. Therefore, if the slot is scheduled for uplink transmission in a given cell, only the HII indicator from the other cells is required. For downlink scheduling, only the RNTP indicator is needed. The weights in the uplink and downlink can be defined as follows: where L_l refers to the number of cells in the same cluster of cell l.

(c) *Resource allocation procedure:* The approach followed and highlighted in Algorithm 1 is based on the suboptimal technique proposed in [26] and the aforementioned definition of the weighting factors. We will show the algorithm for uplink scheduling and using full coordination then discuss the difference for the downlink and cluster coordination cases. In the presented algorithm, $\Gamma_{i,\mathcal{I}_{\mathrm{sub},i}\cup\{j\},l,s}=\sum_{c\in(\mathcal{I}_{\mathrm{sub},i}\cup\{j\})}\Gamma_{i,c,l,s}$. In the expression, $\mathcal{I}_{\mathrm{sub},i,l,s}$ is the set of subcarriers allocated to user i in cell l and slot s. Hence, $\Gamma_{i,\mathcal{I}_{\mathrm{sub},i}\cup\{j\},l,s}$ is the throughput of that user in case subcarrier j is acquired by user i. $\Lambda_{i,j}$ is the marginal utility, which is the main metric to decide the optimised allocation on a given subcarrier and reflects the throughput increase by obtaining a given subcarrier. The presented algorithm assumes equal power allocation among subcarriers, which offers excellent tradeoffs compared with optimal power allocation. Equal power allocation is in fact less computationally complex and requires less information with minimal loss in performance especially in high SNR regimes [27]. For each slot s and cell l, the presented algorithm iterates over all subcarriers and users and selects the user for which the subcarrier provides the highest increase in the utility. This is carried out by calculating the throughput if subcarrier j is allocated to user i (Step 8), finding the throughput with the current set of allocated subcarriers $\mathcal{I}_{\mathrm{sub},i,l,s}$ (Steps 9–13) then calculating the marginal utility (Step 14) and selecting the user that maximises it (Step 16). This subcarrier is finally added to the user's set of allocated subcarriers (Step 17). For the downlink of the full coordination case, the procedure is similar to the one highlighted in Algorithm 1. The only difference is that the power is assumed to be fixed for all users and equal to P_{BS}/K. For cluster coordination, the resource allocation process is similar. The only difference is with the weighting factors. Thus, the resource allocation procedure is generic to all cases. The final results are biased by the choice of the different weighting factors and the selection of the switching point configuration, which was carried out in the second stage.

$$\beta^{\mathrm{cc,U}}_{i,j,l,s}=\left(\prod_{u=1,u\neq l}^{L_l}\left(d_{\mathrm{MS}_{i,l},\mathrm{BS}_u}\right)^{\mathrm{HII}_{j,u}}\right)^{(1/L_l)}\qquad \beta^{\mathrm{cc,D}}_{i,j,l,s}=\left(\prod_{e=1,e\neq l}^{L_l}\left(d_{\mathrm{MS}_{i,l},\mathrm{BS}_e}\right)^{\mathrm{RNTP}_{j,e}}\right)^{(1/L_l)} \tag{21}$$

21613915, 2016, 1, Downloaded from https://onlinelibrary.wiley.com/doi/10.1002/ett.2782 by HINARI-LEBANON, Wiley Online Library on [02/08/2024]. See the Terms and Conditions (https://onlinelibrary.wiley.com/terms-and-conditions) on Wiley Online Library for rules of use; OA articles are governed by the applicable Creative Commons License

Algorithm 1 Uplink Subcarrier Allocation Algorithm

for s such that $1 \leqslant s \leqslant S$ **do**
  for l such that $1 \leqslant l \leqslant L$ and $t(l,s) = 0$ **do**
    for i such that $1 \leqslant i \leqslant M_l^U$ **do**
      $\mathcal{I}_{\text{sub},i} \leftarrow \emptyset$
    end for
    for k such that $1 \leqslant j \leqslant K$ **do**
      for all i such that $1 \leqslant i \leqslant M_l^U$ **do**
        $$\Gamma_{i,\mathcal{I}_{\text{sub},i}\cup\{j\},l,s} \leftarrow \sum_{c\in(\mathcal{I}_{\text{sub},i}\cup\{j\})} \beta^{\text{fc}}_{i,c,l,s} \log\left(1+\frac{P^U_{\max,i}}{|\mathcal{I}_{\text{sub},i}|+1}\gamma^U_{i,c,l,s}\right)$$
        if $\mathcal{I}_{\text{sub},i,l,s} \neq \emptyset$ **then**
          $$\Gamma_{i,\mathcal{I}_{\text{sub},i},l,s} \leftarrow \sum_{c\in\mathcal{I}_{\text{sub},i}} \beta^{\text{fc}}_{i,c,l,s} \log\left(1+\frac{P^U_{\max,i}}{|\mathcal{I}_{\text{sub},i}|}\gamma^U_{i,c,l,s}\right)$$
        else
          $\Gamma_{i,\mathcal{I}_{\text{sub},i},l,s} \leftarrow 0$
        end if
        $\Lambda_{i,j} \leftarrow \Gamma_{i,\mathcal{I}_{\text{sub},i}\cup\{j\},l,s} - \Gamma_{i,\mathcal{I}_{\text{sub},i},l,s}$
      end for
      $i^* \leftarrow \arg\max_i \Lambda_{i,j}$
      $\mathcal{I}_{\text{sub},i^*,l,s} \leftarrow \mathcal{I}_{\text{sub},i^*,l,s} \cup \{j\}$
    end for
  end for
end for

6. RESULTS AND ANALYSIS

In this section, results related to the suboptimal approach are presented and analysed.

For the suboptimal approach presented in Section 5, we consider a network with $L = 30$ BSs that are randomly distributed. Cell boundaries are obtained by using Voronoi tessellations (More details can be found in [25, Chapter 2]). $M = 30$ users are randomly distributed within each cell. We also consider a TDD-OFDMA system with a slotted frame structure where each frame is composed of $S = 10$ slots to be configured for uplink and downlink transmission. We assume subcarrier-based transmission where $K = 90$ subcarriers are available to be allocated to users in the uplink or downlink in a given slot and cell depending on the frame configuration in that cell. The power budget of the users is $P_{\max} = 125$ mW and the power budget of each of the BSs is $P_{\text{BS}} = 30$ W. The channel variations assume the pathloss and fading models described in Section 2. The presented results are obtained by running the suboptimal approach over many iterations then averaging out. The number of iterations depends on the network size, number of users and subcarriers. For most of the results, it is fixed to two. It goes to 20 for Figure 11.

First, we compare the proposed approach with the synchronised solution with and without cell coordination. In the synchronised solution, the switching point configuration is determined on the basis of the aggregate uplink and downlink network traffic loads and the same configuration is used in all cells. Uplink and downlink data traffic are generated using FTP traffic model 1 [28]. This model assumes independent Poisson packet arrival with a fixed packet size of 0.5 MB. For the downlink, the aggregate arrival rate for a given cell is selected from the set $[0.25, 0.5, 1, 1.5, 2, 2.5, 5, 7.5]$. Note that the last two values were added to account for high downlink traffic loads. Uplink traffic load is found by using the generated traffic load and the per-cell downlink to uplink traffic ratio, which in our case is generated randomly. For our approach, we consider the two cases of full coordination where the interference indicators are exchanged between all cells and the cluster-coordination where they are exchanged only within a cluster and thus neglecting the effect of BS–BS and MS–MS interference in the resource allocation process. Note that the synchronisation case is by default fully coordinated because all cells belong to one cluster. Finally, the weight in the distance measure λ is set to 0.99 which places a significant weight on BS–BS interference and provides a fairer comparison with the synchronisation technique, which eliminates all cross-slot interference types (MS–MS and BS–BS).

6.1. Cluster formation

As was mentioned in Section 5.1, the first step involves performing clustering using the HAC algorithm, which groups the BSs with high susceptibility to interference on each other in one cluster. The iterative clustering is illustrated in the dendrogram of Figure 3. The x-axis indicates the cell indices and the y-axis, the distance between the cells. The clustering algorithms produces 12 clusters as demonstrated in Figure 4. The figure shows the

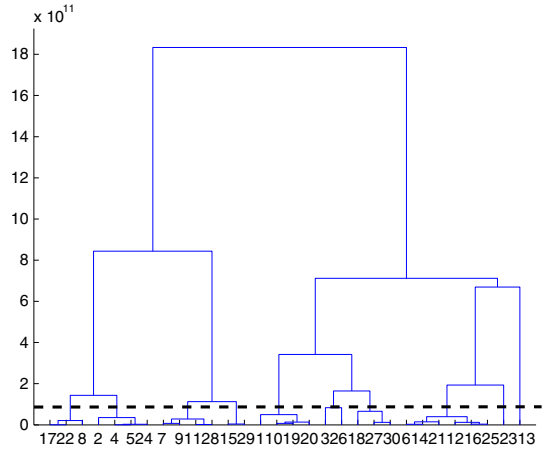

Figure 3. Dendrogram generated by hierarchical agglomerative clustering algorithm. The dashed black line indicates the threshold for cutting the tree.

Trans. Emerging Tel. Tech. **27**:17–33 (2016) © 2014 John Wiley & Sons, Ltd.
DOI: 10.1002/ett

21613915, 2016, 1, Downloaded from https://onlinelibrary.wiley.com/doi/10.1002/ett.2782 by HINARI-LEBANON, Wiley Online Library on [02/08/2024]. See the Terms and Conditions (https://onlinelibrary.wiley.com/terms-and-conditions) on Wiley Online Library for rules of use; OA articles are governed by the applicable Creative Commons License

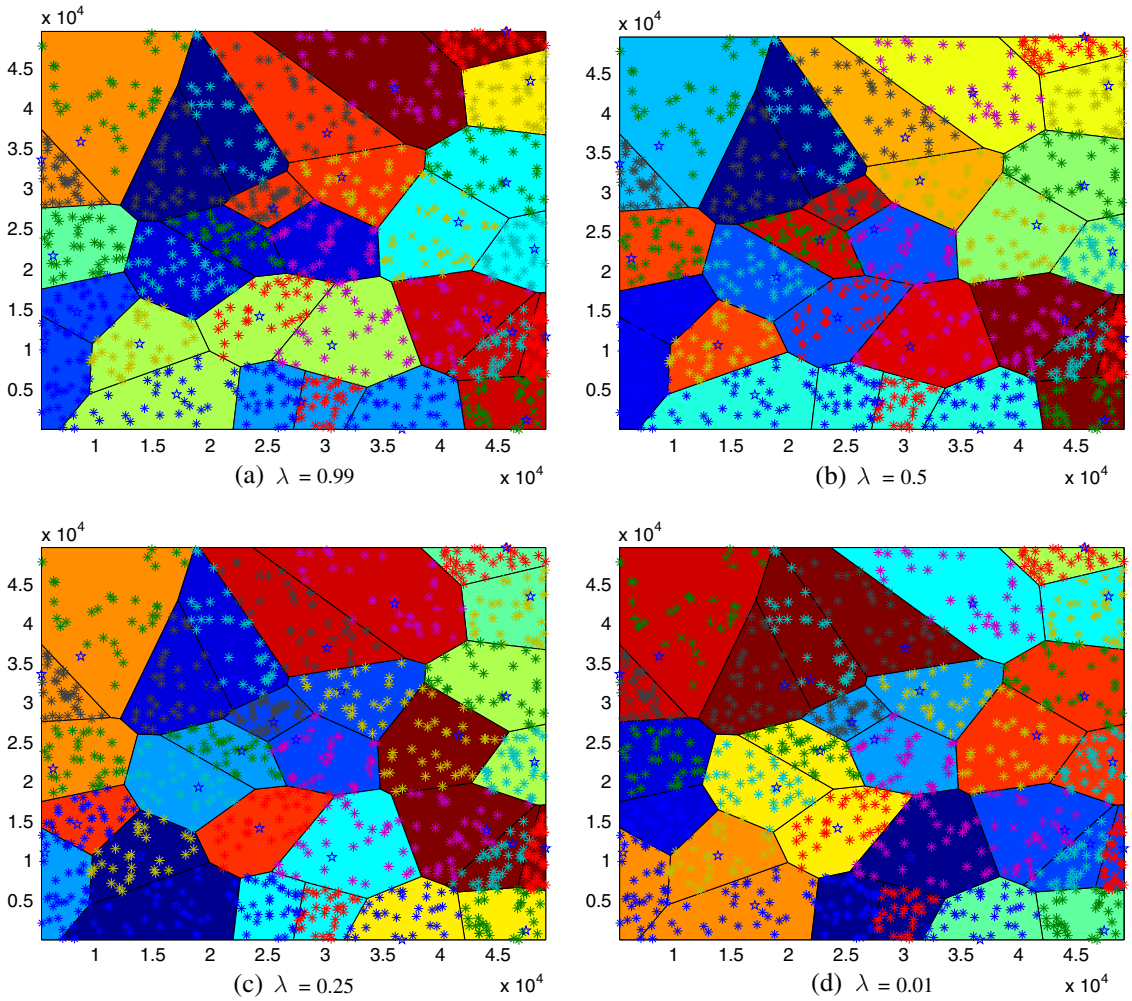

Figure 4. Outcome of the clustering formation stage for different values of the weight λ. Cells with similar colour indicate same cluster membership.

actual network with the randomly placed BSs and users with the colouring reflecting the different clusters produced. The cell boundaries are obtained by drawing the Voronoi tessellations. Each of the subfigures represents the result for a different weighting factor λ.

In fact and as indicated in (17), the clustering depends on the factor λ, which reflects the weight given to the BS–BS and worst case MS–MS interference in the clustering process. Figures 4(a) 4(b), 4(c) and 4(d) show the clustering outcome for values of λ of 0.99, 0.5, 0.25 and 0.01, respectively.

We can note that as the value of λ decreases, the clustering pattern changes from grouping cells where the BSs produce the highest interference and in general cells where the BSs are closest to each other, to grouping cells where the MSs are closest. In the figures, this could be depicted by observing the changes in cell colouring, which indicates modifications to the cluster memberships.

6.2. Switching point configuration

The cluster formation is followed by switching point configuration where the uplink and downlink traffic are taken into consideration to select the best frame structure among the seven LTE frame structures as presented in Figure 2. Note that for convenience in the simulations, the special slots marked with 'S' in Figure 2 are considered for downlink transmission.

Based on the downlink to uplink traffic ratio, the configuration for the synchronised case is as follows:

$$\mathbf{t} = [1, 1, 0, 0, 0, 1, 1, 0, 0, 1] \quad \forall l$$

where 1 indicates downlink transmission and 0 indicates uplink transmission as was used in the optimization formulation. For the clustering approach, the configuration for the 12 clusters is shown in Table II. Compared with the

21613915, 2016, 1, Downloaded from https://onlinelibrary.wiley.com/doi/10.1002/ett.2782 by HINARI-LEBANON, Wiley Online Library on [02/08/2024]. See the Terms and Conditions (https://onlinelibrary.wiley.com/terms-and-conditions) on Wiley Online Library for rules of use; OA articles are governed by the applicable Creative Commons License

Table II. Per-cluster frame structures.

Cluster index \ slot index	1	2	3	4	5	6	7	8	9	10
1	1	1	0	0	0	1	1	1	1	1
2	1	1	0	1	1	1	1	0	1	1
3	1	1	0	0	0	1	1	0	0	0
4	1	1	0	1	1	1	1	0	1	1
5	1	1	0	0	0	1	1	0	0	0
6	1	1	0	1	1	1	1	0	1	1
7	1	1	0	0	0	1	1	1	1	1
8	1	1	0	0	1	1	1	0	0	1
9	1	1	0	1	1	1	1	0	1	1
10	1	1	0	1	1	1	1	0	1	1
11	1	1	0	0	0	1	1	0	0	0
12	1	1	0	1	1	1	1	0	1	1

synchronisation approach, cross-slots exist between cells belong to different clusters, like for instance slots 4 and 5 between clusters 1 and 2. However, because of grouping of the highly interfering cells in the same cluster, the effect of the cross-slot interference is reduced especially for the full coordination case as will be shown in the next section.

6.3. Resource allocation

The final stage after determining the best switching point configuration is to perform multicellular resource allocation. Three main areas are used to compare and analyse the three TDD resource management techniques, namely, the achievable uplink and downlink rates, the interference in the network and finally the adaptation to the traffic variations.

(1) *Rate analysis:* First, the uplink and downlink rates are investigated. Equations (8)–(9) show the intricate dependence of the achievable rate in either direction on the resource allocation and frame structure in the other cells, which determines the interference level and thus directly affects the achievable rates. For our simulated network, the per cell average uplink and downlink rates are presented in Figures 5(a) and 5(b), respectively. Note that the rates are taken per cell. The values obtained are high and may exceed sometimes the peak values in the LTE standard. However, several factors can contribute to these values including the number of subcarriers (90), which is low compared with the value used in actual LTE networks; thus, more power will be spent per subcarrier increasing the achievable rate.

In Figure 5(a), the performance of two variants of the cluster-based resource management scheme is compared with cell synchronisation in the uplink. We can notice that the rate achieved by synchronising transmission across the network is higher than the two clustering approaches. The main reason behind this is that BS–BS interference is totally eliminated and approximately a thousand times higher than MS–BS interference, which is the second kind affecting the uplink rate and this is because of the fact that the pathloss of the BS–BS connection is modelled with an exponent of two, which is nearly twice that of the MS–BS link. The full coordination case comes second. In this technique, the negative effect of the BS–BS interference is leveraged by the clustering

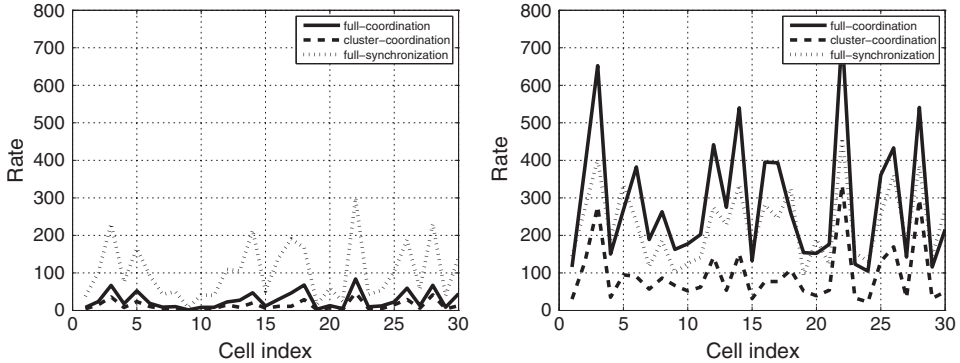

(a) Uplink Rate (b) Downlink Rate

Figure 5. Uplink and downlink rate outcomes of the resource allocation stage for the simulated network (rates in bps/Hz/cell).

Trans. Emerging Tel. Tech. **27**:17–33 (2016) © 2014 John Wiley & Sons, Ltd.
DOI: 10.1002/ett

21613915, 2016, 1, Downloaded from https://onlinelibrary.wiley.com/doi/10.1002/ett.2782 by HINARI-LEBANON, Wiley Online Library on [02/08/2024]. See the Terms and Conditions (https://onlinelibrary.wiley.com/terms-and-conditions) on Wiley Online Library for rules of use; OA articles are governed by the applicable Creative Commons License

approach and the multicellular resource allocation technique adopted. The cluster coordination demonstrates the worst performance because it does not take into account interference information from cells located outside the cluster. These conclusions go along with the findings of the LTE technical specification in [17] where it is mentioned that *'decreased UL packet throughput for macro cells compared with the fixed configuration is observed without any interference mitigation schemes because of severe eNB-to-eNB interference in multi-macro/pico cell scenarios'*. The cluster coordination interference mitigation scheme applied in this paper limits the penalty incurred in the uplink throughput but does not eliminate it completely. This could also be explained that the BS–BS interference is almost 1000 times greater than the MS–BS interference, and thus, the uplink direction is BS–BS limited.

To illustrate this dependence, we consider a picocell-picocell transmission scenario where the transmission loss between two picocells has a pathloss exponent of 4. The results are presented in Figure 6. The obtained uplink throughput is shown in Figure 6(a). As shown, the rate difference in the uplink is smaller than that of the normal BS–BS model in Figure 5(a). The figure demonstrates the shift in the achievable uplink rate. When the pathloss model changes for the BS–BS connection, the clustering is normally altered. Figure 6(a) shows that the gap between the clustering and synchronised case is smaller.

The different approaches are also compared in the downlink as shown in Figure 5(b). In this figure, the performance of the full coordination clustering approach is better than full cell synchronisation. This can be explained by the fact that synchronisation eliminates MS–MS interference at the cost of regular BS–MS interference, which is much larger because the pathloss exponent is lower and the transmit power higher than the former case. For the picocell scenario with a pathloss exponent of 4, the resulting downlink throughput is shown in Figure 6(b).

We can note that the trend remains the same with the proposed approach outperforming network synchronisation. Compared with the case with a regular BS–BS channel model, the achievable downlink rate is nearly the same. The differences can be explained by the change in the clustering outcome due to use of another pathloss exponent.

In general, the decrease of one type of interference dictates the behaviour of the other for each communication link. This results in different achievable rates when the traffic conditions and switching point configurations change. The results of [17] complement this analysis where it is stated that *'The benefits may be observed in either DL or UL or both directions. The less number of DL (or UL) subframes in the fixed reference TDD UL-DL configuration, the higher DL (or UL) packet throughput gain (if any) achieved by TDD UL-DL reconfiguration.'*

In the description of the suboptimal algorithm, it was mentioned that equal power allocation is employed because it has a performance that is close to the optimal power allocation but with lower computational complexity. To investigate the difference of performance, we consider the same scenario but use the waterfilling algorithm instead. The implementation of the algorithm is based on the discussion in [29, Section 9.4]. Figure 7(a) shows the resulting achieved downlink rate when optimal power allocation is performed. Compared with Figure 5(b), the achieved rate in the downlink and for the three approaches is very close. For the same channel conditions and user locations in the two cases, the differences result from a slightly different subcarrier allocation outcome in the cells and a different power allocation approach. Moreover, the channel gains over the different subcarriers are relatively small and close to each other. The optimal allocation outcome turns out to be close to an equal power allocation most of the time. This trend was also observed when

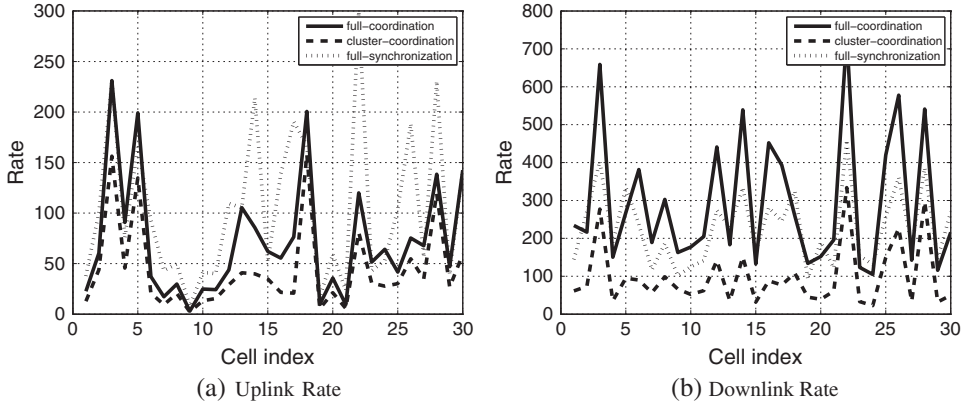

Figure 6. Uplink and downlink rate outcomes of the resource allocation stage for the picocell network (rates in bps/Hz/cell).

21613915, 2016, 1, Downloaded from https://onlinelibrary.wiley.com/doi/10.1002/ett.2782 by HINARI-LEBANON, Wiley Online Library on [02/08/2024]. See the Terms and Conditions (https://onlinelibrary.wiley.com/terms-and-conditions) on Wiley Online Library for rules of use; OA articles are governed by the applicable Creative Commons License

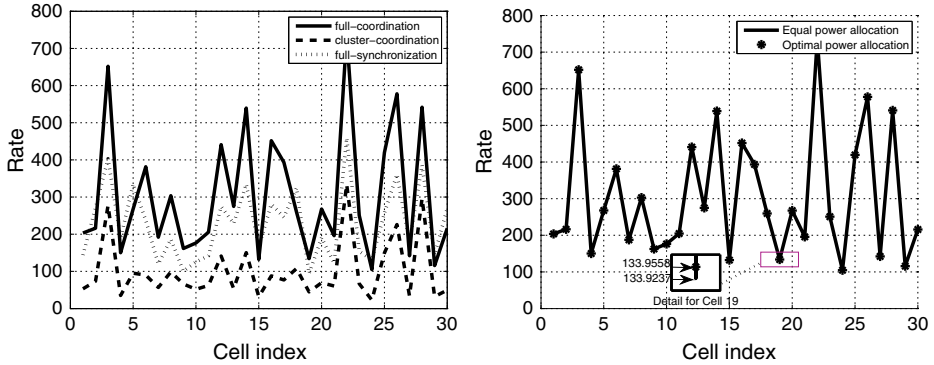

Figure 7. Downlink rate outcome for the three simulated approaches with optimal power allocation (left). Comparison between equal and optimal power allocation for the full coordination case (right).

running the small optimization scenario as described in Section 4.

The closeness of the two power allocations techniques is highlighted in Figure 7(b). As shown, the plots are overlapping indicating a very small difference in the achievable rate. The zoomed subplot shows the downlink rate in cell 19 while employing the two schemes. The difference in the achieved rate is 0.032 bps/Hz, which is very small indicating a very close performance.

(2) *Interference analysis:* To investigate the problem more deeply, we present some results related to the different interference types. Because synchronisation eliminates cross-slots interference, we only include in the comparison of the BS–MS and MS–BS interference types. Figure 8 shows the empirical cumulative distribution function of the BS–MS interference and MS–BS interference. For the BS–MS interference shown in Figure 8(a), we can note that the downlink rate trend in Figure 5(b) coincides with the interference trend where for a given interference value, the cumulative probability of users reaching this value is higher for the cluster approach, which generally reflects lower BS–MS interference per-user in this approach. Also note that the cumulative distribution function for both clustering approaches coincide because of the fact that cluster coordination only neglects cross-slot interference.

In analogy, the same thing can be said about the relation between the uplink rate in Figure 5(a) and the MS–BS cdf plot in Figure 8(b) where this type of interference shows an opposite trend to the BS–MS case. Again, all the statistics depend on the frame configuration in each cell of the networks, and as a result, on the number of cross-slots, the channel conditions on a particular slot and on the resource allocation approach used.

Finally, we compare the BS–BS and MS–MS interference statistics between the three approaches. The reference case is the cell synchronisation approach where the two types of interference have a value of zero. Figure 9 shows the average BS–BS and MS–MS interference per cell. These figures demonstrate that because of the full coordination between cells, the MS–MS and BS–BS interference are very low compared with cluster-coordination,

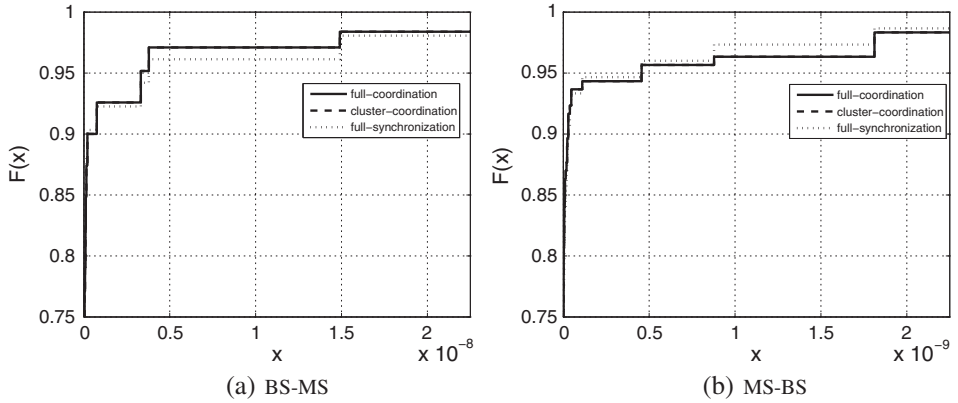

Figure 8. Cumulative Distribution Function of base station (BS)–mobile station (MS) and MS–BS interference.

Trans. Emerging Tel. Tech. **27**:17–33 (2016) © 2014 John Wiley & Sons, Ltd.
DOI: 10.1002/ett

21613915, 2016, 1, Downloaded from https://onlinelibrary.wiley.com/doi/10.1002/ett.2782 by HINARI-LEBANON, Wiley Online Library on [02/08/2024]. See the Terms and Conditions (https://onlinelibrary.wiley.com/terms-and-conditions) on Wiley Online Library for rules of use; OA articles are governed by the applicable Creative Commons License

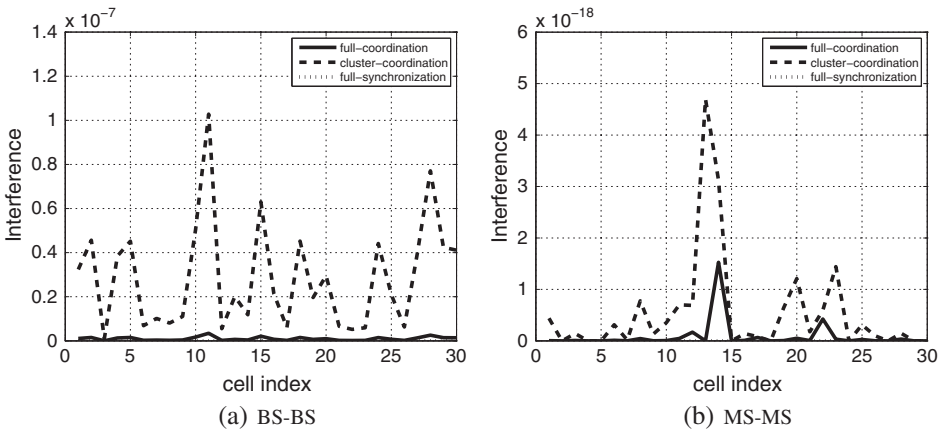

(a) BS-BS (b) MS-MS

Figure 9. Average per-cell base station (BS)–BS and mobile station (MS)–MS interference resulting from applying the three different approaches.

which neglects the effect of cross-slot interference between different clusters. This large surge in these types of interference leads to the worst performance in terms of uplink and downlink throughput. The reduction in the signalling overhead comes at the expense of a drop in performance in the case of a cluster-coordinated network (interference indicators only exchanged within a cluster).

(3) *Traffic adaptation:* Finally, we need to investigate the traffic adaptation of the clustering approach. One indicator is to compare the downlink ratio each cell gets compared with the required one, which is given as the ratio of the traffic volume in the downlink to the total combined traffic volume. The results are presented in Figure 10. We can notice from the figure that downlink ratio configured in the clustered approach follows to a certain extent the required ratio. The differences are because of the fact that the switching point is determined on a cluster basis and not on a cell basis. Moreover, the available options of configurations are limited to the standardised frame structures. On the other hand, cell synchronisation imposes a fixed configuration for all cells. In this simulation, it is a 50 : 50 configuration, which clearly fails to follow the traffic variations.

To assess the level of traffic adaptation, we propose a traffic adaptation index based on the well-known Jain fairness index [30]. The index defined by Jain *et al.* considered the throughput of a wireless channel as follows:

$$\mathcal{J}(x_1, \cdots, x_n) = \frac{\left(\sum_{i=1}^{n} x_i\right)^2}{n \cdot \sum_{i=1}^{n} x_i^2} \tag{22}$$

where n is the number of users and x_i is the throughput of connection i. A value of 1 indicates total fairness.

In this paper, the expression is used to define a traffic adaptation index, which reflects whether the approach followed adapts to the traffic loads in the uplink and downlink. Thus, we define x_l (where the value is per-cell) as follows:

$$x_l = \left| \frac{R_l^U}{R_l^D} - \theta_l \right| \tag{23}$$

where R_l^U, R_l^D are the per-cell average achievable throughputs in the uplink and downlink, respectively, after running the suboptimal algorithm. θ_l is the ratio of uplink to downlink traffic volumes in cell l. Figure 11 shows the resulting index for the proposed approach as well as the synchronised network solution for different per-cell user loads. This figure demonstrates that the proposed approach offers better traffic adaptation capabilities, and this is because of the fact that the switching point configurations are synchronised at a cluster level where each cluster usually contains at most five cells. Moreover, the index changes from a user load to the other. This is mainly because of the second stage in the suboptimal algorithm where the average uplink and downlink loads in a cluster are used to determine the switching point configuration in that cluster (the aggregate

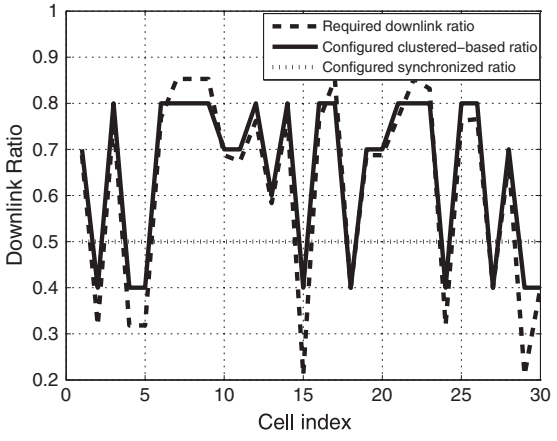

Figure 10. Required and configured downlink ratio.

21613915, 2016, 1, Downloaded from https://onlinelibrary.wiley.com/doi/10.1002/ett.2782 by HINARI-LEBANON, Wiley Online Library on [02/08/2024]. See the Terms and Conditions (https://onlinelibrary.wiley.com/terms-and-conditions) on Wiley Online Library for rules of use; OA articles are governed by the applicable Creative Commons License

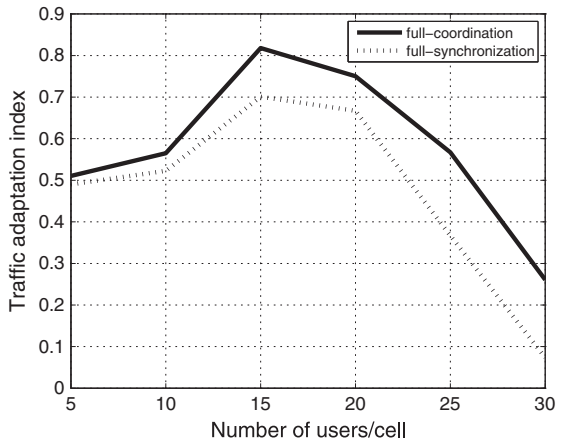

Figure 11. Traffic adaptation index variation with different per-cell user loads.

uplink and downlink traffic are considered). This could result in one cluster member having a different switching point configuration to the one that corresponds to its uplink to downlink traffic ratio.

In summary, the result has shown that the proposed clustered approach represents an intermediate solution between full synchronisation and dynamic adaptation. More noticeably, the full coordination clustering approach is able to reduce BS–BS and MS–MS interference to a very low level close to the synchronised case. However, the presence of a BS–BS interference limits the performance a bit in the uplink, and this is mainly because of the low loss in the BS–BS channel (pathloss exponent of 2). On the other hand, the downlink performance is very good and exceeds that of full synchronisation. This is mainly because of the fact that the effect of MS–MS interference is small compared with the BS–MS counterpart. As far as traffic adaptation is concerned, the relatively small size of the clusters compared with the full network size allows better traffic adaptation because the penalty of synchronisation is limited to a few cells.

7. CONCLUSIONS

In this paper, the problem of joint switching point configuration and resource allocation was formulated as an MINLP problem. The problem was further linearized to reduce the complexity. To cope with large network sizes, a suboptimal framework is proposed. Clustering is first performed to group highly interfering cells and synchronise transmission therin. Then switching point configuration is performed on the basis of the per-cell uplink and downlink traffic volumes. Finally, multicellular resource allocation is performed. Simulation results show the flexibility of the approach and the good trade-off it offers between interference mitigation and traffic adaptation. In particular, the proposed approach allows a good adaptation of the switching point configuration to the varying traffic loads while maintaining the interference values at an acceptable level compared with the synchronisation technique, which eliminates sources of high interference (e.g., BS–BS) at the expense of poor dynamic traffic adaptation.

ACKNOWLEDGEMENTS

This work was made possible by NPRP grant 4-347-2-127 from the Qatar National Research Fund (a member of The Qatar Foundation). The statements made herein are solely the responsibility of the authors.

REFERENCES

1. Chan P, Lo E, Wang R, Au E, Lau V, Cheng R, Mow W, Murch R, Letaief KB. The evolution path of 4G networks: FDD or TDD? *IEEE Communications Magazine* 2006; **44**(12): 42–50.
2. Janis P, Ribeiro C, Koivunen V. Flexible UL-DL switching point in TDD cellular local area wireless networks. *Springer Mobile Networks and Applications* 2012; **17**(5): 695–707.
3. Ghimire B, Auer G, Haas H. Busy bursts for trading off throughput and fairness in cellular OFDMA-TDD. *EURASIP Journal on Wireless Communications and Networking* 2009; **2009**: 1–14.
4. Ghimire B, Auer G, Haas H. OFDMA-TDDnetworks with busy burst enabled grid-of-beam selection, *IEEE ICC*, 2009.
5. Liu Y, Tao M, Lin B, Shen H. Optimization framework and graph-based approach for relay-assisted bidirectional OFDMA cellular networks. *IEEE Transactions on Wireless Communications* 2010; **9**(11): 3490–3500.
6. Foutekova E, Sinanovic S, Haas H. Asymmetry balancing for channel asymmetry support in OFDMA-TDD cellular networks. In *IEEE Vehicular Technology Conference, VTC-Fall*, Calgary, Alberta, Canada, September 2008.
7. Zhu E, Huo J, Zho S, Zeng Z, Ding W. An adaptive resource allocation scheme in OFDMA based multiservice WiMAX systems. In *International Conference on Advanced Communication Technology, ICACT*, Gangwon-Do, Korea, February 2008.
8. Kumar D, Chellappan C. Adaptive slot management for OFDMA based cellular wireless networks in TDD mode. *Journal of Theoretical and Applied Information Technology* 2009; **5**(6): 686–692.
9. Chiang C-H, Liao W, Liu T. Adaptive downlink/uplink bandwidth allocation in IEEE 802.16 (WiMAX) wireless networks: A cross-layer approach. In *IEEE Global Telecommunications Conference, GLOBECOM'07*, Washington DC, USA, November 2007.

21613915, 2016, 1, Downloaded from https://onlinelibrary.wiley.com/doi/10.1002/ett.2782 by HINARI-LEBANON, Wiley Online Library on [02/08/2024]. See the Terms and Conditions (https://onlinelibrary.wiley.com/terms-and-conditions) on Wiley Online Library for rules of use; OA articles are governed by the applicable Creative Commons License

10. Kou M, Zhen Y. Dynamic uplink/downlink resource allocation for TDD OFDMA access network. In *International Conference on Communications and Mobile Computing*, Kunming, Yunnan, China, January 2009.
11. Chahed T, Elayoubi S-E, Altman E. On design of TDD for joint uplink and downlink resource allocation in OFDMA-based WiMAX. In *IEEE Vehical Technology Conference VTC-Fall*, Calgary, Alberta, Canada, September 2008.
12. Kim J, Choi B-G, Bae S, Doh I, Chung M. Adaptive time division duplexing configuration mode selection mechanism for accommodating asymmetric traffic in time division long term evolution-advanced systems. *Transactions on Emerging Telecommunications Technologies* 2013; **24**(3): 342–351.
13. Shen Z, Khoryaev A, Eriksson E, Pan X. Dynamic uplink-downlink configuration and interference-management in TD-LTE. *IEEE Communications Magazine* 2012; **50**(11): 51–59.
14. Holma H, Toskala A. *Lte for UMTS: Evolution to LTE-Advanced*. Wiley: Chichester, United Kingdom, 2011.
15. El-Hajj AM, Dawy Z. Dynamic joint switching point configuration and resource allocation in TDD-OFDMA wireless networks. In *IEEE Global Telecommunications Conference, GLOBECOM'11*, Houston Texas, USA, December 2011.
16. Sesia S, Toufik I, Baker M. *LTE the UMTS Long Term Evolution* (2nd ed.) Wiley: Chichester, United Kingdom, 2011.
17. 3GPP Technical Specification Group. TS 36.828 V11.0.0: Further enhancements to LTE time division Duplex (TDD) for downlink-uplink (DL-UL) interference management and traffic adaptation (release 11). *Technical Report*, 3GPP, Sophia-Antipolis Cedex, France, 2012.
18. Floudas C, Pardalos P. *Encyclopedia of Optimization*. Springer: New York, NY, 2009.
19. Ghezavati V, Saidi-Mehrabad M. An efficient linearization technique for mixed 01 polynomial problem. *Elsevier Journal of Computational and Applied Mathematics* 2011; **235**: 1730–1738.
20. Duran M, Grossman I. An outer approximation algorithm for a class of mixed-integer nonlinear programs. *Math Program* 1986; **36**: 307–339.
21. Hunting M. The AIMMS outer approximation algorithm for MINLP (using GMP functionality). *White Paper*, Paragon Decision Technology, 2011.
22. 3GPP Technical Specification Group. TS 36.423 V11.4.0: X2 application protocol, X2AP (release 11). *Technical Report* , 3GPP, Sophia-Antipolis Cedex, France, 2013.
23. Romney M. *LTE and the Evolution to 4G Wireless: Design and Measurement Challenges* (2nd ed.) Wiley: Chichester, United Kingdom, 2013.
24. 3GPP Technical Specification Group. TS 36.211 V11.2.0: Physical channels and modulation (release 11). *Technical Report*, 3GPP, Sophia-Antipolis Cedex, France, 2013.
25. Theodoridis S, Koutroumbas K. *Pattern Recognition* (4th ed.) Academic Press: San Diego, California, 2009.
26. Yaacoub E, Dawy Z. *Resource Allocation in Uplink OFDMA Wireless Systems*. Wiley: Hoboken, New Jersey, 2012.
27. Tse D, Viswanath P. *Fundamentals of Wireless Communications*. Cambridge University Press: New York, 2005.
28. 3GPP Technical Specification Group. TS 36.814 V9.0.0: Further advancements for E-UTRA physical layer aspects (release 9). *Technical Report*, 3GPP, Sophia-Antipolis Cedex, France, 2010.
29. Cover T, Thomas J. *Elements of Information Theory* (2nd ed.) Wiley: Hoboken, New Jersey, 2006.
30. Jain R, Chiu D, Hawe W. A quantitative measure of fairness and discrimination for resource allocation in shared computer systems. *Technical Report DEC Research Report TR-301*, Digital Equipment Corporation, Hudson, MA, 1984.

21613915, 2016, 1, Downloaded from https://onlinelibrary.wiley.com/doi/10.1002/ett.2782 by HINARI-LEBANON, Wiley Online Library on [02/08/2024]. See the Terms and Conditions (https://onlinelibrary.wiley.com/terms-and-conditions) on Wiley Online Library for rules of use; OA articles are governed by the applicable Creative Commons License